

Journal of Materials Chemistry A

Accepted Manuscript



This is an *Accepted Manuscript*, which has been through the Royal Society of Chemistry peer review process and has been accepted for publication.

Accepted Manuscripts are published online shortly after acceptance, before technical editing, formatting and proof reading. Using this free service, authors can make their results available to the community, in citable form, before we publish the edited article. We will replace this *Accepted Manuscript* with the edited and formatted *Advance Article* as soon as it is available.

You can find more information about *Accepted Manuscripts* in the [Information for Authors](#).

Please note that technical editing may introduce minor changes to the text and/or graphics, which may alter content. The journal's standard [Terms & Conditions](#) and the [Ethical guidelines](#) still apply. In no event shall the Royal Society of Chemistry be held responsible for any errors or omissions in this *Accepted Manuscript* or any consequences arising from the use of any information it contains.

Cite this: DOI: 10.1039/c0xx00000x

www.rsc.org/xxxxxx

ARTICLE TYPE

Improvement of Photovoltaic Performance of DSSCs by Modifying Panchromatic Zinc Porphyrin Dyes with Heterocyclic Units

Hai-Lang Jia,^a Ze-Min Ju,^a Hong-Xia Sun,^b Xue-Hai Ju,^c Ming-Dao Zhang,^d Xing-Fu Zhou^b and He-Gen Zheng^{*a}

Received (in XXX, XXX) Xth XXXXXXXXX 20XX, Accepted Xth XXXXXXXXX 20XX
DOI: 10.1039/b000000x

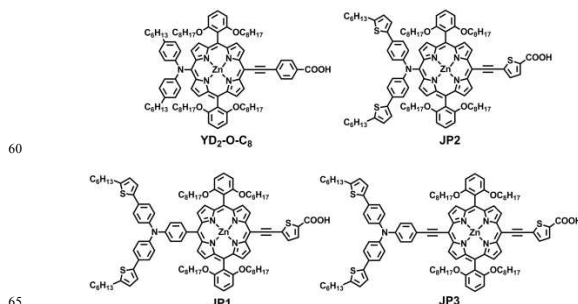
Dedicated to Professor Xin-Quan Xin on the occasion of his 80th birthday.

A series of novel panchromatic D-D- π -A porphyrin dyes have been synthesized and applied to dye-sensitized solar cells. Three porphyrin dyes named JP1, JP2 and JP3, their photophysical, electrochemical properties and photovoltaic performance were investigated and compared with reference dye YD2-O-C8. The 2-hexylthiophene chromophores were introduced to the donor groups, which extended the π -conjugation system effectively, then broaden the range of spectral response and improved the charge separation between the donor and acceptor moieties in the excited state. Moreover, this paper used thiophene-2-carboxylic acid instead of the traditional benzoic acid as anchor groups, which can make the molecules arrange to tilted orientation when adsorbed on TiO₂ surface, and this may effectively suppress the dye aggregation and prevent charge recombination. These dyes were clearly red-shifted when compared with dye YD2-O-C8. Especially for dye JP3, its maximum absorption peak was red shifted 20 nm than that for dye YD2-O-C8 from 645 to 665 nm, and the molar extinction coefficient ($6.2 \times 10^4 \text{ M}^{-1} \text{ cm}^{-1}$) of JP3 is the double of YD2-O-C8 ($3.1 \times 10^4 \text{ M}^{-1} \text{ cm}^{-1}$) at Q band. The dye JP3 extended the spectral response to 750 nm. The density function theory (DFT) calculations indicated that the electronic density of the HOMO was increased by the additional thiophene units in these dyes when compared with YD2-O-C8, and this will improve the conjugation and electron donating ability. The power conversion efficiency of JP1, JP2 and JP3 are 5.09%, 5.62% and 6.40% respectively under AM 1.5G irradiation, which reaching 74.5%, 82.3% and 93.7% of the YD2-O-C8 based-device (6.83%) under the same conditions.

1. Introduction

Dye-sensitized solar cells (DSSCs) have received widespread attention due to their low costs, ease of fabrication and high power conversion efficiency (PCE).^{1,2} Since reported by Grätzel in 1991,³ DSSCs have made great progress and have been regarded as a promising photovoltaic technology to solve the global energy crisis. Although the power conversion efficiency of ruthenium-based dyes have surpassed 10%, but ruthenium complexes are difficult to synthesis and the rare metal ruthenium is very expensive.⁴⁻⁶ Currently, many researchers are devoted to developing new and efficient sensitizers such as porphyrin dyes^{7,8} or metal-free organic dyes^{9,10} to substitute ruthenium-based dyes. Generally, most sensitizers are often designed to donor- π -acceptor (D- π -A) architecture,¹¹⁻¹³ which is conducive to improving intramolecular charge transfer (ICT) and tailoring bandgap energy. It has been found that the donor groups such as triarylamine, carbazole, indoline, phenoxazine and tetrahydroquinoline¹⁴⁻¹⁶ in conjunction with different acceptor groups such as ethynylbenzoic acid, phosphoric acid, sulphonic acid and pyridine^{17,18} can construct low band gap sensitizers for

DSSCs. Inspired by this strategy, many new architectures including D-D- π -A, D-A- π -A and D- π -A- π -A¹⁹⁻²¹ have been explored. The power conversion efficiency of 12.3% has been achieved through co-sensitized by porphyrin dye YD2-O-C8 and organic dye Y123 with cobalt-based redox electrolyte.²² Recently, Grätzel research group synthesized dye SM315 by introduced benzothiadiazole (BTD) between the porphyrin ring and acceptor, and the power conversion efficiency of 13% was achieved.²³ This indicates that the molecular engineering of panchromatic sensitizers is one of the most direct and effective ways to improve the PCE of DSSCs.²⁴



Schem 1 Chemical structures of YD2-O-C8, JP1, JP2 and JP3

Porphyrin sensitizers have broad absorption at the Soret (400-450 nm) and Q bands (550-600 nm).^{25,26} If we further improve their absorption intensity, broaden the range of the spectral response by use of some chromophores, or introduce long alkyl chains to block the π - π stacking and reduce charge recombination, then the overall performance of the DSSCs will get a lot of improvement. Many researchers often optimize the donor segments by introducing rich electronic chromophores, or extending the length of the π -conjugated segments to improve the light-harvesting performance of the dye molecules.²⁷ In our previous reports,^{28,29} we have succeeded in introducing suitable heterocyclic groups to triarylamine dyes which effectively extend the scope of spectral absorption. The thiophene units with lone pair electrons can effectively delocalize the positive charges and extend the π -conjugation system, which have been widely applied in organic polymer solar cells.³⁰ In this work, we introduced 2-hexylthiophene to the donor groups and used thiophene-2-carboxylic acid as anchor groups. Introduction of the bulky side chain and thiophene chromophores on the periphery of starburst triphenylamine or diphenylamine is one of effective strategies to suppress dye aggregation and extend the effective conjugation length. The dye aggregation is also affected by the dye's geometry and resulting arrangement on the TiO₂ surface.³¹ By the geometry optimization, the thiophene-2-carboxylic acid induces tilted oriented dye geometry when it binds to TiO₂ surface for dye JP1-JP3 compared with dye YD2-O-C8, this will help suppress dye aggregation and prevent I₃⁻ of the electrolyte penetrating into the TiO₂ surface. We found that the absorption ranges of JP2 and JP3 were obviously red-shifted and the JP3 based-device showed superior charge transport properties. Scheme 1 shows the chemical structures of YD2-O-C8, JP1, JP2 and JP3. We further characterize the photophysical, electrochemical properties and photovoltaic performance of the dyes.

2. Experimental

Synthesis and characterizations of dyes

The synthetic routes of JP1, JP2 and JP3 are depicted in Scheme 2. The compounds 2-5 were synthesized by Suzuki coupling reaction or Sonogashira coupling reaction, the compound 6 was synthesized according ref. 22. The compound 7 was obtained by Buchwald-Hartwig coupling of compound 2 and compound 6, compound 8 was obtained by Suzuki coupling of compound 5 and compound 6, and compound 9 was obtained by Sonogashira coupling of compound 4 and compound 6. Finally, Sonogashira coupling of compounds 7-9 and thiophene-2-carboxylic acid to give JP1-JP3.

Fabrication of DSSCs

The working electrode (active area 0.16 cm²) was prepared by screen printing the TiO₂ paste on Fluorine-doped tin oxide (FTO) glass plates (15 Ω /square). The TiO₂ paste consisted of 12 μ m thick film (particle size, 20 nm, pore size 32 nm). Then the electrode were immersed into 0.2 mM dye (YD2-O-C8, JP1, JP2 and JP3) solution in a mixture of toluene and ethanol (toluene/ethanol = 1/1) for 18 h. The working electrode and the Pt counter electrode were then sealed with a Surlyn film (25 μ m) by heating the sandwich-type cell at 110°C. The electrolyte was introduced through pre-drilled holes in the counter electrode and

was driven into the cell via vacuum backfilling, the hole was sealed with a Surlyn film and a thin glass (0.1 mm thickness) cover by heating.³² Al foil was taped at the back side of each counter electrode to reflect unabsorbed light. The electrolyte was composed of 0.6 M 1-butyl-3-methylimidazolium iodide (BMII), 30 mM I₂, 50 mM LiI, 0.5 M tert-butylpyridine and 0.1 M guanidiniumthiocyanate (GuNCS) in a solvent mixture of acetonitrile and valeronitrile (volume ratio, 85:15).

Characterizations of DSSCs

The photocurrent-voltage (*I-V*) curves of the DSSCs were measured on a Keithley 2400 source meter under standard global AM 1.5G solar irradiation supplied by a xenon light source (Oriel). The incident photo-to-electron conversion efficiency (IPCE) spectra of the DSSCs were measured by a DC method. The light source was a 300 W xenon lamp (Oriel 6258) coupled with a flux controller to improve the stability of the irradiance. The single wavelength was selected by a monochromator (Cornerstone 260 Oriel74125). Light intensity was measured by a NREL traceable Si detector (Oriel 71030NS) and the short circuit currents of the DSSCs were measured by an optical power meter (Oriel 70310).

Theoretical calculations

In order to investigate the geometrical configuration and electron distribution of YD2-O-C8, JP1, JP2 and JP3, density function theory (DFT) calculations were performed at the DFT-B3LYP/LanL2MB level with Gaussian 09 suite of programs.

UV-Vis spectroscopy, Photoluminescence, ATR-FTIR spectra, Electrochemical properties and Measurement of dye adsorbed amounts

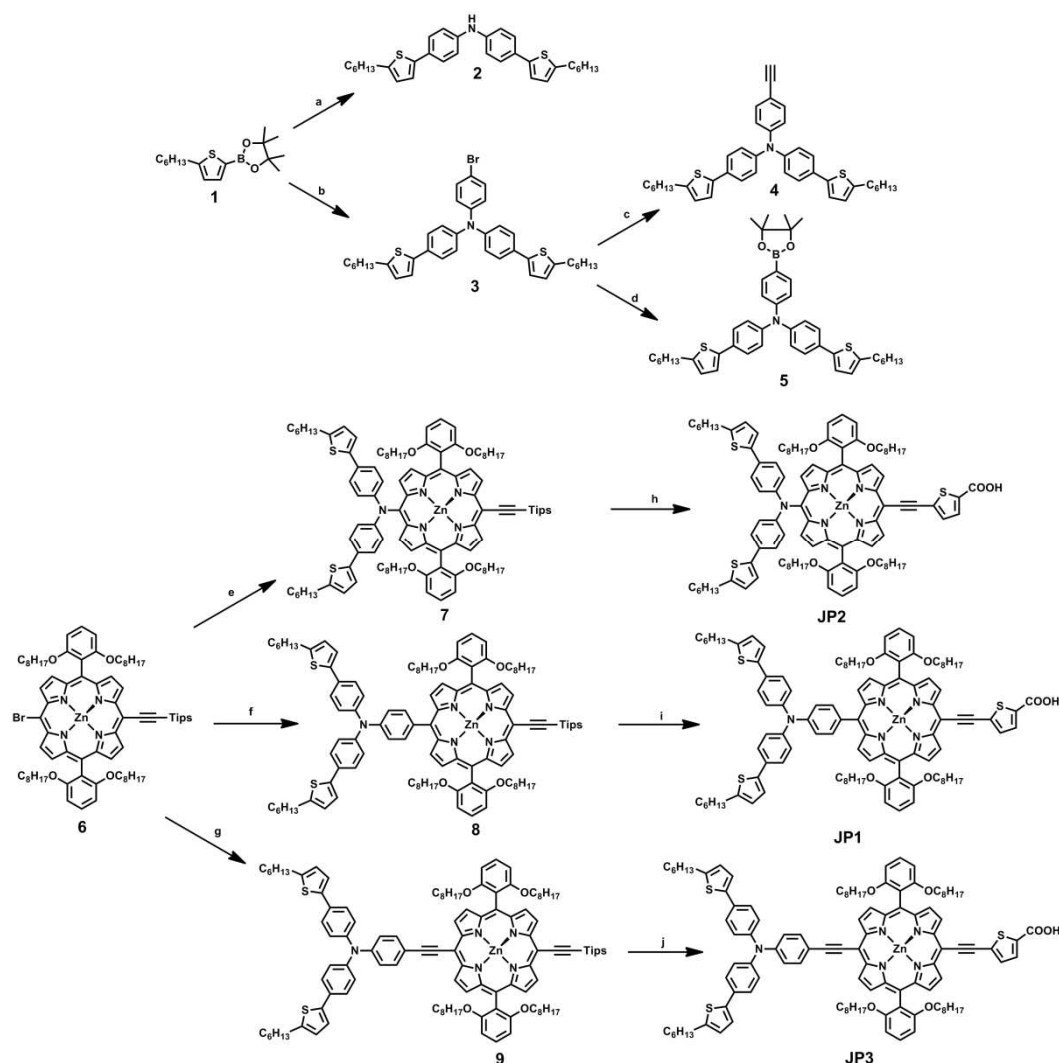
UV-vis absorption spectra were recorded on a Shimadzu UV-3600 spectrometer. Fluorescence spectra were recorded on a Perkin Elmer LS55 spectrophotometer. ATR-FTIR spectra were recorded on a Vector22 spectrometer. The fluorescence lifetimes of the dyes were measured on a FLS920 spectrometer. Quasi-reversible oxidation and reduction waves were recorded on a Chenhua CHI660D model Electrochemical Workstation (Shanghai). Electrochemical Impedance Spectroscopy were studied using a Chenhua CHI660I model Electrochemical Workstation (Shanghai).

The dye adsorbed amounts on the TiO₂ films were measured by a Shimadzu UV-3600 spectrometer. The sensitized 4×4 mm electrodes were immersed into a 0.1 M NaOH solution in a mixed solvent (water/ethanol = 1/1), which resulted in the desorption of each dye.

3. Results and discussion

Absorption and Emission Spectroscopy

The UV-Vis absorption spectra of YD2-O-C8, JP1, JP2 and JP3 examined in THF are shown in Fig. 1, and the corresponding data are collected in Table 1. The four dyes exhibit typical porphyrin absorption characteristics at the Soret and Q bands. The absorption at 400-700 nm can be attributed to electronic transitions from π - π^* and the intramolecular charge transfer (ICT). The maximum absorption peaks of JP1, JP2 and JP3 are respectively red-shifted 5, 5 and 10 nm when compared with dye



Scheme 2 synthesis procedure of **JP1**, **JP2** and **JP3**. Reagents and conditions: a) Bis(4-bromophenyl)amine, Pd(PPh₃)₄, K₂CO₃, H₂O, 1, 4-dioxane, 90 °C; b) Tris(4-bromophenyl)amine, Pd(PPh₃)₄, K₂CO₃, H₂O, 1, 4-dioxane, 90 °C; c) i: Trimethylsilylacetylene, Pd(PPh₃)₂Cl₂, CuI, TEA, 80 °C; ii: TBAF, THF, rt; d) Bis(pinacolato)diboron, Pd(dppf)Cl₂, KOAc, DMF, 80 °C; e) Compound 2, NaH, DPEphos, Pd(OAc)₂, toluene, reflux; f) Compound 5, Pd(PPh₃)₄, K₂CO₃, H₂O, 1, 4-dioxane, 90 °C; g) Compound 4, Pd₂(dba)₃, AsPh₃, TEA, THF, reflux; h) i: TBAF, THF, rt; ii: 5-bromothiophene-2-carboxylic acid, Pd₂(dba)₃, AsPh₃, TEA, THF, reflux; i) i: TBAF, THF, rt; ii: 5-bromothiophene-2-carboxylic acid, Pd₂(dba)₃, AsPh₃, TEA, THF, reflux; j) i: TBAF, THF, rt; ii: 5-bromothiophene-2-carboxylic acid, Pd₂(dba)₃, AsPh₃, TEA, THF, reflux.

YD2-O-C8 at Soret band. Apparently, the 2-hexylthiophene units extend the conjugative delocalization with the diphenylamine or triphenylamine segment. Especially for JP1, it not only has a red shift, but also has a higher molar extinction coefficient ($2.89 \times 10^5 \text{ M}^{-1} \text{ cm}^{-1}$) when compared with YD2-O-C8 ($2.20 \times 10^5 \text{ M}^{-1} \text{ cm}^{-1}$) at Soret band, which owing to adding a benzene ring is favour of extending the conjugative delocalization. Though, the relatively nonplanar structure of dye JP1 may weaken the intramolecular charge transfer, so it is blue shifted 10 nm at Q band compared with YD2-O-C8. The spectral response of JP3 is broader and stronger than the other dyes at Q band, which due to the rigid C=C may extend the π -conjugation system, decrease the HOMO-LUMO gap and improve the charge transfer from donor to acceptor. The maximum absorption peak of JP3 is red shifted 20 nm than that for dye YD2-O-C8 from 645 to 665 nm, and the molar extinction coefficient ($6.2 \times 10^4 \text{ M}^{-1} \text{ cm}^{-1}$) of JP3 is the double of YD2-O-C8 ($3.1 \times 10^4 \text{ M}^{-1} \text{ cm}^{-1}$) at Q band. Their major

emission bands are 659, 675, 684 and 672 nm for JP1, JP2, JP3 and YD2-O-C8 respectively (Fig. S1, ESI†). It is similar to the trend of the absorption spectra of the four dyes.

The UV-Vis absorption spectra of these dyes adsorbed onto TiO₂ are shown in Fig. 1b. The absorption ranges of the four dyes are all broadened and their maximum absorption peaks are slightly blue shifted after anchoring onto TiO₂, and might be due to deprotonation of the carboxylic acid.³³ It was also investigated by attenuated total reflectance fourier-transform infrared spectroscopy (ATR-FTIR). Such as JP3 (Fig. 2), when it is adsorbed on TiO₂, the ATR-FTIR spectra show carbonyl stretch $\nu(\text{C}=\text{O})$ disappears at 1654 cm^{-1} , with a concomitant increase at 1380 cm^{-1} which originates from the symmetric carboxylate band $\nu(\text{COO}^-)$. It is characteristic of bidentate binding by both oxygen atoms of the carboxylate functional group to the titania of the substrate. The results indicate that JP3 adsorbed on the TiO₂ surface by dehydration reactions.

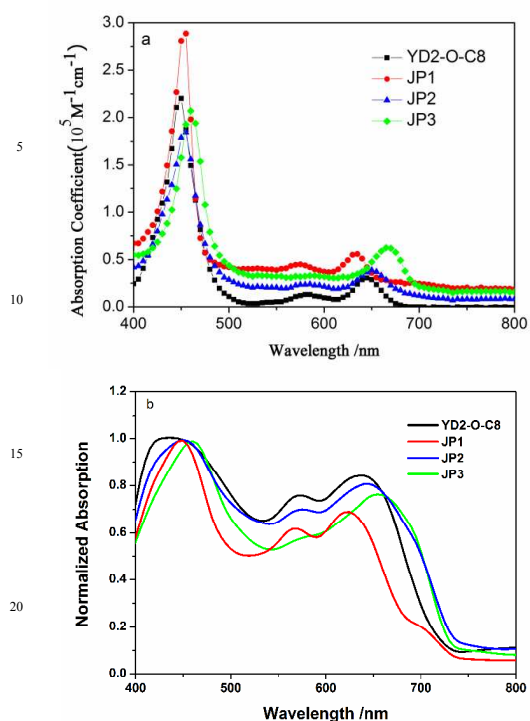


Fig. 1 (a) UV-Vis absorption spectra of YD2-O-C8, JP1, JP2 and JP3 in THF (b) Absorption spectra of the dyes anchoring on the 12 μm porous TiO₂ nanoparticle film.

Table 1 Absorption and emission properties of dyes in THF

Dye	Absorption ^a		Emission ^a	
	$\lambda_{\text{max}}/\text{nm}$ ($\epsilon \times 10^5 \text{ M}^{-1}\text{cm}^{-1}$)		$\lambda_{\text{max}}/\text{nm}$	lifetime ^b / ns
JP1	455(2.89), 570(0.44), 635(0.56)		659	2.34, 9.16
JP2	455(1.84), 585(0.24), 650(0.39)		675	1.70, 7.21
JP3	460(2.07), 570(0.32), 665(0.62)		684	1.72, 6.21
YD2-O-C8	450(2.20), 580(0.13), 645(0.31)		672	1.78, 6.79

^aAbsorption, emission spectra and emission lifetime were measured in tetrahydrofuran solution ($1 \times 10^{-6} \text{ M}$), ^bFluorescence decay curves of dyes are shown in Fig. S2. ESI†

Electrochemical Studies

Electrochemical properties of these dyes were investigated by cyclic voltammogram (Fig. 3). The optical transition energies (E_{0-0}) were estimated from the absorption onset. The ground state oxidation potentials (E_{ox}) of YD2-O-C8, JP1, JP2 and JP3 are all quasi-reversible, with values of 0.828, 0.955, 0.825 and 0.773 V vs. normal hydrogen electrode (NHE), respectively. The oxidation of JP3 is cathodically shifted by 0.182 V relative to JP1, indicating elevated energy levels are caused by extended π -conjugation system. Their E_{ox} are all more positive than the redox potential of the I^-/I_3^- couple (0.4 V vs. NHE), indicating the oxidized dye can easily get electrons for effective regeneration. The excited oxidation potentials (E_{ox}^*) of the dyes

can be calculated by the formula $E_{\text{ox}}^* = E_{\text{ox}} - E_{0-0}$. The E_{0-0} of YD2-O-C8, JP1, JP2 and JP3 are 1.851, 1.759, 1.698 and 1.653 eV, respectively. The excited oxidation potentials (E_{ox}^*) of YD2-O-C8, JP1, JP2 and JP3 are -1.023, -0.804, -0.873 and -0.880 V, respectively. They are all more negative than the conduction band of TiO₂ (-0.5 V vs. NHE). These suggest that such a condition is required for the effective injection of electron from the excited dye into the conduction band of TiO₂. The fluorescence lifetime of the dye was also investigated (Fig. S2, Table 1), and the nanosecond lifetime indicated the excited dyes have enough time to complete the electron injection process.

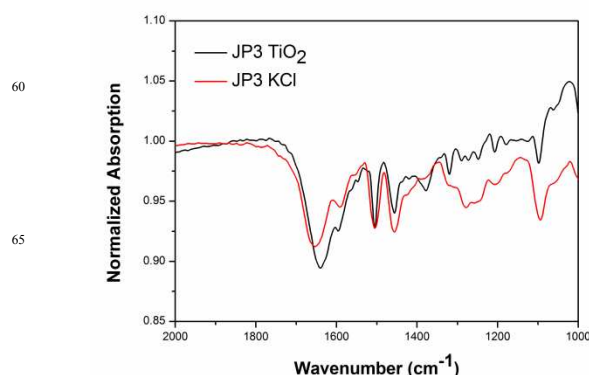


Fig. 2 ATR-FTIR spectra of dye powders (red line) and dyes adsorbed on TiO₂ nanoparticles (black line) for dye JP3

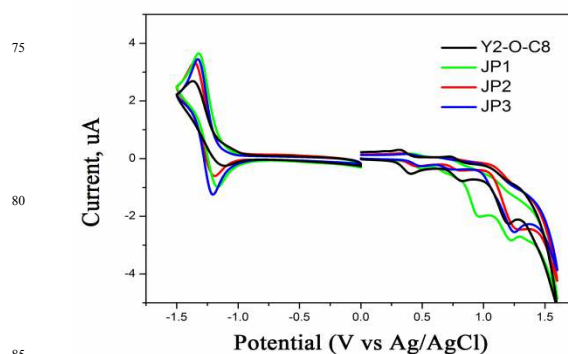


Fig. 3 Cyclic voltammogram of YD2-O-C8, JP1, JP2 and JP3 in DMF (0.1 M TBAPF₆, glassy carbon electrode as working electrode, Pt as counter electrode, Ag/Ag⁺ as reference electrode, scan rate: 100 mV s⁻¹)

Theoretical Calculations

The HOMOs and LUMOs of YD2-O-C8, JP1, JP2 and JP3 are shown in Fig. 4. The HOMO of YD2-O-C8 is populated over the diphenylamine and porphyrin ring, whereas the HOMOs of JP1-JP3 mainly are populated over the thiophene units and arylamine units, and partly are populated over the porphyrin rings. It is clear that the thiophene units can make contribution to the HOMOs of the three dyes due to its rich electronic properties. The LUMO is essentially spread over the porphyrin ring and the thiophene-2-carboxylic acid anchor groups. Such a well-separated orbital distribution is in favor of the separation of photoexcitation charge, and that suggests the photoinduced charge can be efficiently injected from excited dyes to the conduction band of TiO₂.²²

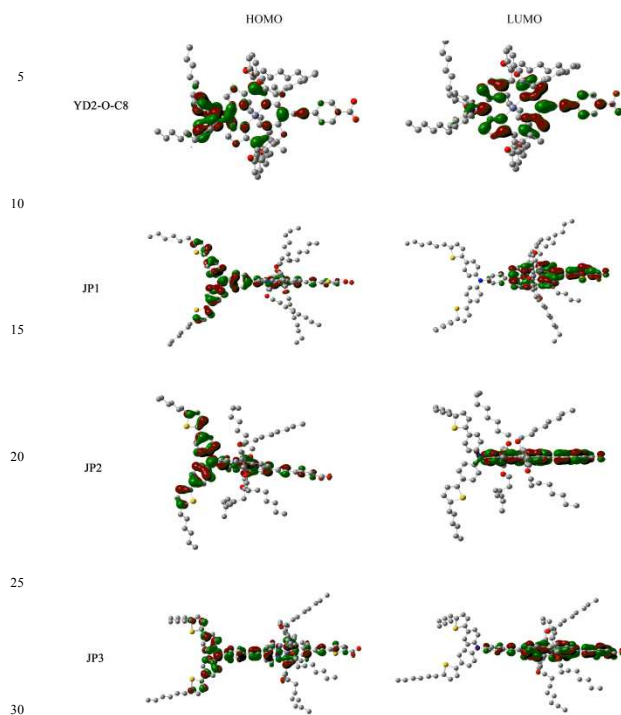


Fig. 4 HOMOs and LUMOs frontier molecular orbitals of **YD2-O-C8**, **JP1**, **JP2** and **JP3** calculated by density-functional theory (DFT) at the DFT-B3LYP/LanL2MB level with Gaussian 09 suite of programs.

Photovoltaic Performance of DSSCs

DSSC experiments have been performed, the photovoltaic performance parameters are listed in Table 2, and the I-V curves of the DSSCs are shown in Fig. 5. The YD2-O-C8 based-device has the highest power conversion efficiency (η) of 6.83%, the η of JP3 (6.40%) is higher than JP1 (5.09%) and JP2 (5.62%). Their fill factors have no much difference. The open-circuit photovoltage (V_{oc}) of JP3 (0.692 V) is higher than YD2-O-C8 (0.683 V), JP1 (0.664 V) and JP2 (0.655 V), it is mainly due to its better charge transport properties for excellent π -conjugation system. By the geometry optimization, as depicted in Fig. 6, it showed the thiophene-2-carboxylic acid acceptor can make the molecules arrange to tilted orientation when adsorbed on TiO_2 surface,^{34,35} and this may effectively suppress the aggregation of dye molecules and prevent I_3^- of the electrolyte penetrating into the TiO_2 surface. The dihedral between the triphenylamine and the porphyrin macrocycle is 72° for JP1 (Fig. S3), which indicates that it has a relatively nonplanar structure, that in favour of reducing the charge recombination, hence the V_{oc} of JP1 is higher than JP2. The short-circuit density (J_{sc}) of these DSSCs decreased in the order of YD2-O-C8 (15.20 mA cm⁻²) > JP3 (13.67 mA cm⁻²) > JP2 (12.61 mA cm⁻²) > JP1 (11.36 mA cm⁻²), it is consistent with the incident photo-to-electron conversion efficiency (IPCE) spectra (Fig. 5b). The IPCE values of JP3 exceed 60% from 425 to 475 nm and attain 70% at 450 nm at Soret band. Apparently, the IPCE curve of JP3 is higher and broader than the other three dyes at Q band, which is attributed to

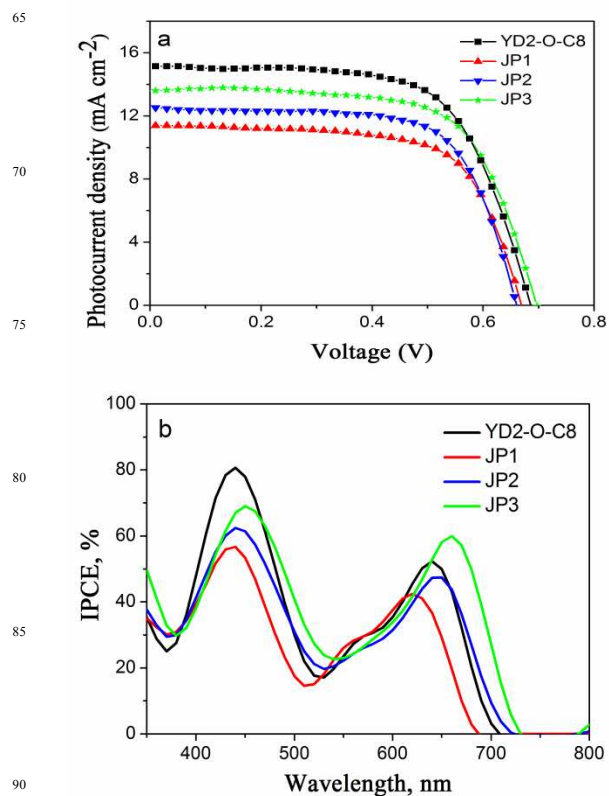


Fig. 5 (a) Current-voltage characteristics of DSSCs based on **YD2-O-C8**, **JP1**, **JP2** and **JP3** under standard global AM 1.5G solar irradiation. (b) IPCE spectra of DSSCs based on **YD2-O-C8**, **JP1**, **JP2** and **JP3** under standard global AM 1.5G solar irradiation

Table 2 Photovoltaic parameters of the DSSCs obtained from the I-V curves

Dye	J_{sc} (mA cm ⁻²)	V_{oc} (V)	FF (%)	η (%)	Dye adsorbed amounts (10 ⁻⁸ mol cm ⁻²)
YD2-O-C8	15.20	0.683	65.8	6.83	4.72
JP1	11.36	0.664	67.4	5.09	3.30
JP2	12.61	0.655	68.0	5.62	6.25
JP3	13.67	0.692	67.6	6.40	4.11

The size of the active area for each cell is 0.16 cm², the DSSCs were all measured under standard global AM 1.5G solar irradiation. Al foil was taped at the back side of each counter electrode to reflect unabsorbed light.



Fig. 6 Anchoring unit affects the dye JP3's orientation on the TiO_2 surface

its broader absorption and high molar extinction coefficient in the visible region. The IPCE curves of JP1 and JP2 are lower and narrower than JP3, especially for JP1, its lower J_{sc} and IPCE reduce the overall performance of DSSCs. The IPCE values of YD2-O-C8 exceed 70% from 417 to 461 nm and attain 80% at 440 nm, so YD2-O-C8 has the highest J_{sc} . In order to further research the J_{sc} of the DSSCs, the adsorption amounts of these dyes were also investigated (Table 2). The value of JP1 (3.30×10^{-8} mol cm^{-2}) is less than JP2 (6.25×10^{-8} mol cm^{-2}), JP3 (4.11×10^{-8} mol cm^{-2}) and YD2-O-C8 (4.72×10^{-8} mol cm^{-2}), it may be an important reason for the low J_{sc} of JP1.

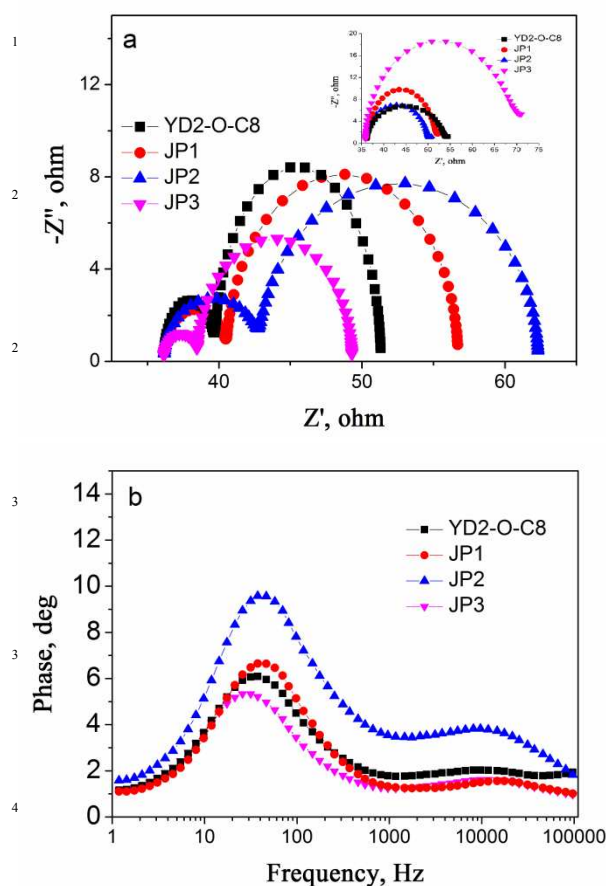


Fig. 7 (a) Nyquist plots observed under illumination, the inset displayed the Nyquist plots under dark, (b) Bode phase plots under illumination, scanned from 10^5 to 1 Hz, the applied potential was set at the open circuit condition and 5 mV.

Electrochemical Impedance Spectroscopy

Electrochemical impedance spectroscopy (EIS) is a useful tool to investigate the interfacial charge transfer processes in DSSCs.³⁶ The electrochemical impedance spectroscopy was measured under illumination and under dark. The Nyquist plots and Bode phase plots are shown in Fig. 7. For the Nyquist plots under illumination,³⁷ two semicircles were observed, the large semicircle corresponds to the charge-transfer resistance (R_{ct}) at the $\text{TiO}_2/\text{dye}/\text{electrolyte}$ interface, and the small semicircle corresponds to the transport resistance at $\text{Pt}/\text{electrolyte}$. The radii

of the large semicircle increase in the order of $\text{JP3} < \text{YD2-O-C8} < \text{JP1} < \text{JP2}$, which indicate the JP3 has the smallest charge-transfer resistance. The result is consistent with the V_{oc} of the DSSCs. A high performance DSSCs has lower charge-transfer resistance, which is advantageous to collect electron and enhance photocurrent. The smallest R_{ct} of JP3 indicates that the electron collection efficiency is better than the other DSSCs. For the Nyquist plots under dark (the inset of Fig. 7a), the large semicircle corresponds to the electron recombination at the $\text{TiO}_2/\text{dye}/\text{electrolyte}$ interface. The JP3 based-device has the largest semicircle suggests it has a highest charge recombination resistance, this is helpful for the suppression of dark current. Hence, the V_{oc} of JP3 is higher than the other DSSCs, it is consistent with the previous reports. The Bode phase plots (Fig. 7b) shows the frequency peaks of the charge transfer process at different interfaces.³⁸ The middle frequency related to the charge recombination rate. The lower frequency corresponded to the larger charge recombination resistance and longer electron lifetime. The middle frequency of the DSSCs follows the order: $\text{JP3} < \text{YD2-O-C8} < \text{JP1} < \text{JP2}$, which is consistent with V_{oc} of the DSSCs.

4. Conclusions

In conclusion, we have developed a novel approach of introducing 2-hexylthiophene chromophores to porphyrin dyes and using thiophene-2-carboxylic acid instead of the traditional benzoic acid as anchor groups. Introduction of the bulky side chain hexyl and thiophene chromophores on the periphery of starburst triphenylamine or diphenylamine is one of effective strategies to suppress dye aggregation and extend the effective conjugation length. The thiophene-2-carboxylic acid induces tilted oriented dye geometry when it binds to TiO_2 surface for dye JP1-JP3, and this will help suppress dye aggregation and prevent I_3^- of the electrolyte penetrating into the TiO_2 surface. The dye JP3 extends the spectral response to 750 nm and the JP3 based-device has a higher power conversion efficiency (η) of 6.40%, which is slightly lower than YD2-O-C8 (6.83%) under the same conditions. The results will provide guidance for the synthesis of high performance dyes to improve the power conversion efficiency of DSSCs.

Acknowledgements

This work was supported by grants from the Natural Science Foundation of China (Nos. 21371092; 21401107), National Basic Research Program of China (2010CB923303), Natural Science Foundation of Jiangsu Province, China (No. BK20140986).

Notes and references

- ^aState Key Laboratory of Coordination Chemistry, School of Chemistry and Chemical Engineering, Nanjing National Laboratory of Microstructures, Nanjing University, Nanjing 210093, P. R. China, E-mail: zhenghg@nju.edu.cn. Fax: 86-25-83314502.
^bState Key Laboratory of Materials-Oriented Chemical Engineering, College of Chemistry and Chemical Engineering, Nanjing University of Technology, Nanjing 210009, P. R. China, E-mail: zhouxf@njut.edu.cn.
^cSchool of Chemical Engineering, Nanjing University of Science and Technology, Nanjing 210094, P. R. China, E-mail: xhju@mail.njust.edu.cn.

- ^dJiangsu Key Laboratory of Atmospheric Environment Monitoring and Pollution Control, School of Environmental Science and Engineering, Nanjing University of Information Science & Technology, Nanjing 210044, Jiangsu, P.R. China. E-mail: matchlessjimmy@163.com.
- ⁵ † Electronic supplementary information (ESI) available: synthesis details and characterization data; Fig. S1-S3 showing emission spectra, fluorescence decay curves and the geometry optimized ground state molecular structures. See DOI: 10.1039/b000000x/
- 1 L. L. Li, E. W. G. Diau, *Chem. Soc. Rev.*, 2013, **42**, 291-304.
- 10 2 A. Hagfeldt, G. Boschloo, L. C. Sun, L. Kloo and H. Pettersson, *Chem. Rev.*, 2010, **110**, 6595-6663.
- 3 B. O'Regan, M. Grätzel, *Nature*, 1991, **353**, 737-740.
- 4 M. K. Nazeeruddin, A. Kay, I. Rodicio, R. Humphry-Baker, E. Miiller, P. Liska, N. Vlachopoulos and M. Grätzel, *J. Am. Chem. Soc.*, 1993, **115**, 6382-6390.
- 15 5 D. Kuang, C. Klein, S. Ito, J. E. Moser, H. B. Robin, N. Evans, F. Durliaux, C. Grätzel, S. M. Zakeeruddin and M. Grätzel, *Adv. Mater.*, 2007, **19**, 1133-1137.
- 6 Q. J. Yu, Y. H. Wang, Z. H. Yi, N. N. Zu, J. Zhang, M. Zhang and P. Wang, *ACS Nano.*, 2010, **4**, 6032-6038.
- 20 7 Y. J. Liu, N. Xiang, X. M. Feng, P. Shen, W. P. Zhou, C. Weng, B. Zhao and S. T. Tan, *Chem. Commun.*, 2009, **18**, 2499-2501.
- 8 C. P. Hsieh, H. P. Lu, C. L. Chiu, C. W. Lee, S. H. Chuang, C. L. Mai, W. N. Yen, S. J. Hsu, E. W. G. Diau and C. Y. Yeh, *J. Mater. Chem.*, **2010**, **20**, 1127-1134.
- 25 9 J. H. Yum, P. Walter, S. Huber, D. Rentsch, T. Geiger, F. Nuesch, F. De Angelis, M. Grätzel and M. K. Nazeeruddin, *J. Am. Chem. Soc.*, 2007, **129**, 10320-10321.
- 10 N. S. F. Risplendi, D. Pugliese, S. Bianco, A. Sacco, A. Lamberti, R. Gazia, E. Tresso and G. Cicero, *J. Phys. Chem. C.*, 2013, **117**, 22778-22783.
- 30 11 X. M. Ren, S. H. Jiang, M. Y. Cha, G. Zhou and Z. S. Wang, *Chem. Mater.*, 2012, **24**, 3493-3499.
- 12 L. H. Yu, J. Y. Xi, H. T. Chan, T. Su, L. J. Antrobus, B. Tong, Y. P. Dong, W. K. Chan and D. L. Phillips, *J. Phys. Chem. C.*, 2013, **117**, 2041-2052.
- 35 13 C. J. Jiao, N. J. Zu, K. W. Huang, P. Wang and J. S. Wu, *Org. Lett.*, 2011, **13**, 3652-3655.
- 14 W. D. Zeng, Y. M. Cao, Y. Bai, Y. H. Wang, Y. S. Shi, M. Zhang, F. Wang, C. Y. Pan and P. Wang, *Chem. Mater.*, 2010, **22**, 1915-1925.
- 40 15 Z. Q. Wang, X. F. Wang, D. Yokoyama, H. Sasabe, J. Kido, Z. Y. Liu, W. J. Tian, O. Kitao, T. Ikeuchi and S. I. Sasaki, *J. Phys. Chem. C.*, 2014, **118**, 14785-14794.
- 16 A. Venkateswararao, K. R. J. Thomas, C. P. Lee, C. T. Li and K. C. Ho, *Appl. Mater. Interfaces.*, 2014, **6**, 2528-2539.
- 45 17 Q. J. Yu, Y. H. Wang, Z. H. Yi, N. N. Zu, J. Zhang, M. Zhang and P. Wang, *ACS Nano.*, 2010, **4**, 6032-6038.
- 18 W. J. Youngblood, S. H. A. Lee, Y. Kobayashi, E. A. Hernandez-Pagan, P. G. Hoertz, T. A. Moore, A. L. Moore, D. Gust and T. E. Mallouk, *J. Am. Chem. Soc.*, 2009, **131**, 926-927.
- 50 19 W. H. Zhu, Y. Z. Wu, S. T. Wang, W. Q. Li, X. Li, J. Chen, Z. S. Wang and H. Tian, *Adv. Funct. Mater.*, 2011, **21**, 756-763.
- 20 W. L. Ding, D. M. Wang, Z. Y. Geng, X. L. Zhao and Y. F. Yan, *J. Phys. Chem. C.*, 2013, **117**, 17382-17398.
- 55 21 K. Panthi, R. M. Adhikari and T. H. Kinstle, *J. Phys. Chem. A.*, 2010, **114**, 4542-4549.
- 22 A. Yella, H. W. Lee, H. N. Tsao, C. Yi, A. K. Chandiran, M. K. Nazeeruddin, E. W. G. Diau, C. Y. Yeh, S. M. Zakeeruddin and M. Grätzel, *Science*, 2011, **334**, 629-633.
- 60 23 S. Mathew, A. Yella, P. Gao, R. Humphry-Baker, B. F. E. Curchod, N. Ashari-Astani, I. Tavernelli, U. Rothlisberger, M. K. Nazeeruddin and M. Grätzel, *Nature Chemistry*, 2014, **6**, 242-247.
- 24 R. M. Ma, P. Guo, H. J. Cui, X. X. Zhang, M. K. Nazeeruddin and M. Grätzel, *J. Phys. Chem. A.*, 2009, **113**, 10119-10124.
- 65 25 Q. Wang, W. M. Campbell, E. E. Bonfantani, K. W. Jolley, D. L. Officer, P. J. Walsh, K. Gordon, R. Humphry-Baker, M. K. Nazeeruddin and M. Grätzel, *J. Phys. Chem. B.*, 2005, **109**, 15397-15409.
- 26 C. W. Lee, H. P. Lu, C. M. Lan, Y. L. Huang, Y. R. Liang, W. N. Yen, Y. C. Liu, Y. S. Lin, E. W. G. Diau and C. Y. Yeh, *Chem. Eur. J.*, 2009, **15**, 1403-1412.
- 27 M. Zhang, Y. L. Wang, M. F. Xu, W. T. Ma, R. Z. Li and P. Wang, *Energy Environ. Sci.*, 2013, **6**, 2944-2949.
- 28 M. D. Zhang, H. Pan, X. H. Ju, Y. J. Ji, L. Qin, H. G. Zheng and X. F. Zhou, *Phys. Chem. Chem. Phys.*, 2012, **14**, 2809-2815.
- 75 29 M. D. Zhang, H. X. Xie, X. H. Ju, L. Qin, Q. X. Yang, H. G. Zheng and X. F. Zhou, *Phys. Chem. Chem. Phys.*, 2013, **15**, 634-641.
- 30 J. A. Christians, R. C. M. Fung and P. V. Kamat, *J. Am. Chem. Soc.*, 2013, **135**, 14960-14963.
- 31 B. G. Kim, K. Chung and J. Kim, *Chem. Eur. J.*, 2013, **19**, 5220-5230.
- 80 32 S. Ito, T. N. Murakami, P. Comte, P. Liska, C. Grätzel, M. K. Nazeeruddin and M. Grätzel, *Thin Solid Films*, 2008, **516**, 4613-4619.
- 33 N. Shibayama, H. Ozawa, M. Abe, Y. Ooyamac and H. Arakawa, *Chem. Commun.*, 2014, **50**, 6398-6401.
- 34 H. Imahori, Y. Matsubara, H. Iijima, T. Umeyama, Y. Matano, S. Ito, M. Niemi, N. V. Tkachenko and H. Lemmetyinen, *J. Phys. Chem. C.*, **2010**, **114**, 10656-10665.
- 85 35 L. P. Si, H. S. He and K. Zhu, *New J. Chem.*, 2014, **38**, 1565-1572.
- 36 F. Fabregat-Santiago, J. Bisquerta, G. Garcia-Belmontea, G. Boschloo and A. Hagfeldt, *Solar Energy Materials & Solar Cells*, **2005**, **87**, 117-131.
- 90 37 K. Mahmood, H. J. Sung, *J. Mater. Chem. A.*, 2014, **2**, 5408-5417.
- 38 A. Baheti, K. R. J. Thomas, C. P. Lee, C. T. Li and K. C. Ho, *J. Mater. Chem. A.*, 2014, **2**, 5766-5779.

Table of contents entry

With a wide spectral response, the η of JP3 based-device reached 6.40% under full sunlight.

